

An Efficient Global Optimization Algorithm with Adaptive Estimates of the Local Lipschitz Constants

Danny D'Agostino

*Department of Industrial Systems Engineering and Management,
National University of Singapore.

Corresponding author(s). E-mail(s): dannydag@nus.edu.sg;

Abstract

In this work, we present a new deterministic partition-based Global Optimization (GO) algorithm that uses estimates of the local Lipschitz constants associated with different sub-regions of the domain of the objective function. The estimates of the local Lipschitz constants associated with each partition are the result of adaptively balancing the global and local information obtained so far from the algorithm, given in terms of absolute slopes. We motivate a coupling strategy with local optimization algorithms to accelerate the convergence speed of the proposed approach. In the end, we compare our approach HALO (Hybrid Adaptive Lipschitzian Optimization) with respect to popular GO algorithms using hundreds of test functions. From the numerical results, the performance of HALO is very promising and can extend our arsenal of efficient procedures for attacking challenging real-world GO problems. The Python code of HALO is publicly available on GitHub.*

Keywords: Global Optimization, Lipschitz Optimization, Black-box Optimization

*<https://github.com/dannyzx/HALO>

1 Introduction

In this work, we consider the following optimization problem

$$\begin{aligned} & \min_{\mathbf{x}} f(\mathbf{x}) \\ & \text{subject to: } \mathbf{x} \in \mathcal{D} \end{aligned} \tag{1}$$

where $f : \mathbb{R}^N \rightarrow \mathbb{R}$, $\mathbf{x} \in \mathbb{R}^N$ and \mathcal{D} is the feasible region of \mathbb{R}^N , defined by box constraints $\mathcal{D} = \{\mathbf{x} \in \mathbb{R}^N : \mathbf{l} \leq \mathbf{x} \leq \mathbf{u}\}$. The N -dimensional vectors \mathbf{l} and \mathbf{u} represent the lower and upper bound on the decision variable \mathbf{x} .

Global optimization (GO) is a critical field in operations research, focusing on methodologies and algorithms for finding the global optimal solution to Problem 1. The pursuit of finding the global optimum covers many scientific disciplines due to its fundamental importance. Extensive academic research has been dedicated to GO, resulting in a plethora of proposed approaches. Stochastic and Evolutionary algorithms, such as Controlled Random Search [1], Genetic Algorithm [2], Simulated Annealing [3], Particle Swarm Optimization [4], and Covariance Matrix Adaptation Evolutionary Strategy (CMA-ES) [5], have proven effective in numerous real-world applications. Another class of GO algorithms involves constructing response surfaces of the objective function using statistical models like Gaussian Processes [6, 7] or Radial Basis Functions [8, 9]. These methodologies exhibit significant performance improvements in scenarios where evaluating the objective function f is computationally expensive.

Lipschitz optimization, extensively studied and developed over the past decades [10–14], constitutes another class of GO algorithms. In Lipschitz optimization, the objective function f is assumed to be Lipschitz continuous on the feasible domain \mathcal{D} . This implies the existence of a constant $0 < L < \infty$ such that

$$|f(\mathbf{x}) - f(\bar{\mathbf{x}})| \leq L \|\mathbf{x} - \bar{\mathbf{x}}\| \quad \forall \mathbf{x}, \bar{\mathbf{x}} \in \mathcal{D} \tag{2}$$

where L represents the global Lipschitz constant of the function f , and $\|\cdot\|$ denotes the Euclidean norm (alternative norms can be utilized, as explored in [15]). The requirement for f to be Lipschitz-continuous is not overly restrictive, as this class encompasses a wide range of functions. For instance, any continuously differentiable function defined within a convex and compact set is Lipschitz continuous [14], with L corresponding to the maximum norm of the gradient $L = \max_{\mathbf{x} \in \mathcal{D}} \|\nabla f(\mathbf{x})\|$. Leveraging the Lipschitz continuity of the objective function f is particularly useful, as it allows for the computation of valid lower bounds across the domain \mathcal{D} . By knowing the function value at a point $f(\bar{\mathbf{x}})$, it becomes possible to compute the lower bound for any $\mathbf{x} \in \mathcal{D}$ that satisfies the following inequality

$$f(\bar{\mathbf{x}}) - L \|\mathbf{x} - \bar{\mathbf{x}}\| \leq f(\mathbf{x}) \tag{3}$$

Exploiting this information algorithmically enables the design of efficient numerical procedures for seeking the global optimum solution to Problem 1.

2 Related Work

During the years, researchers developed Lipschitz optimization methods as in [16, 17] that given the value of the Lipschitz constant L , can produce valid lower bounds of the objective function f and driving the numerical procedure towards the global minimizers.

The difficulty is when the value L of the Lipschitz constant is not available in advance such as in the majority of real-world applications. To effectively overcome this issue, an estimation of it is usually carried out given the information acquired by the optimization procedure during its iterations as in [12].

One popular method that circumvents the need for estimating the Lipschitz constant L is the DIRECT (DIviding RECTangles) algorithm [18]. This derivative-free, partition-based algorithm operates under the determination of *potentially optimal rectangles*, where any value of the global Lipschitz constant L within the range $(0, \infty)$ is implicitly considered during the selection of the partitions to explore. DIRECT possesses several noteworthy features, including a simple partition scheme, an everywhere-dense property that ensures convergence towards the global optimal solution as the algorithm iterates indefinitely, and a minimal number of hyperparameters. In fact, DIRECT has only one hyperparameter and has exhibited robustness in practical applications [18]. These characteristics have inspired the development of several similar algorithms based on the concept of potentially optimal partitions [19–26].

Other efficient and noteworthy algorithms in the Lipschitz optimization class focus on estimating the local Lipschitz constant L_i for each sub-region \mathcal{D}_i of the domain \mathcal{D} . In [27], an algorithm is proposed for optimizing univariate functions, while for multivariate functions, a dimensionality reduction method employing Peano curves is utilized [28, 29]. The estimation of local Lipschitz constants is employed in an efficient diagonal partition-based algorithm described in [30]. In [31], the computation of local Lipschitz constants is integrated into a scheme that reduces the initial multidimensional problem to a set of recursively and adaptively connected univariate subproblems, as further explored in [32]. A similar concept is proposed when the first derivative is available in [33]. However, it is worth noting that the performance of these approaches is highly sensitive to a reliability parameter that users must define beforehand, as emphasized in [30, 31, 34].

Furthermore, successful hybridizations have been achieved by combining some of the aforementioned approaches with local optimization methods. For instance, the DIRECT algorithm has been hybridized with a truncated Newton method in [35] and a coordinate descent approach in [36], resulting in improved performance, as also observed in the methodology presented in [21].

3 Main Contribution

In this work, we present a novel GO algorithm that incorporates an adaptive procedure for estimating the local Lipschitz constant associated with each partition \mathcal{D}_i . Our estimation is obtained through a convex combination of the absolute variation of the objective function around the partition \mathcal{D}_i and the current estimate of the global Lipschitz constant L . The coefficients in the convex combination are dynamically

computed based on the size of the partition \mathcal{D}_i , eliminating the need for users to define any crucial hyperparameters in advance.

We propose a criterion for selecting the most promising partitions based on the information provided by the local Lipschitz constants. This criterion deviates from the concept of potentially optimal hyperrectangles employed in the DIRECT algorithm. Furthermore, we establish the asymptotic convergence of our algorithm called HALO (Hybrid Adaptive Lipschitzian Optimization) to a global minimum, ensuring the everywhere dense property. To expedite the convergence speed of HALO towards stationary points, we introduce a simple coupling strategy with two different local optimization algorithms [37, 38], which we provide motivation for.

Beyond its optimization capabilities, HALO provides the opportunity to gain valuable insights from the black-box objective function. Upon terminating the optimization process, we show that HALO allows the extraction of information about the variables that most significantly influenced the variation of the objective function. This feature is particularly important in scenarios where problem interpretation is necessary.

We evaluate the performance of HALO by comparing it to popular GO algorithms such as DIRECT [18], CMA-ES [5], and the hybridization of DIRECT known as DIRMIN [36]. To assess the algorithms, we conduct an extensive numerical campaign using well-known test functions collected from [39], as well as two additional test function generators specifically designed for GO problems presented in [40, 41]. In total, we consider over one thousand test functions.

The numerical results demonstrate that HALO exhibits strong competitiveness and significantly enhances our arsenal of efficient procedures for tackling challenging real-world GO problems.

4 HALO: Hybrid Adaptive Lipschitzian Optimization

Before delving into the detailed workings of HALO, it is necessary to provide an overview of its main steps and introduce some notation. Algorithm 1 provides a high-level description of the HALO algorithm, outlining its main components and the flow of operations as it consists of three parts: a main program, a selection step, and a partitioning step.

The **Main** function, which takes the maximum number of iterations (**MaxIter**) and the box domain (\mathcal{D}) as input, serves as the main entry point of the algorithm. In line 2, the algorithm begins with a loop over the iterations k . Within this loop, the **Selection** function is called in line 3 to select partitions based on certain criteria (not yet specified). The selected partitions are represented by the subset of indices \mathcal{I}_k^* obtained from the set of indices \mathcal{I}_k , where each index i_k corresponds to a partition \mathcal{D}_{i_k} at iteration k . Lines 4 and 5 contain two nested 'for' loops. The outer loop iterates over each index i_k^* of the selected partitions, while the inner loop (line 5) performs J function evaluations within each partition. The function evaluations are carried out at points $\mathbf{x}_{i_k^*}^j$ sampled from the partition $\mathcal{D}_{i_k^*}$. The corresponding function values $f(\mathbf{x}_{i_k^*}^j)$ are computed using the **Fun_Eval**. Once the inner loop completes, the set $\mathcal{D}_{i_k^*}$ is divided into J non-overlapping subsets (line 14), denoted as $\mathcal{D}_{i_k^*}^j$ for $j = 1, \dots, J$. In line 15, the set of indices \mathcal{I}_k is updated to include the new indices resulting from the

Algorithm 1: General Partition Algorithm for GO

```
1 function main(max_iter,  $\mathcal{D}$ )
2   for  $k$  to max_iter do
3      $\mathcal{I}_k^* \leftarrow \text{selection}(\mathcal{I}_k)$ 
4     for  $i_k^*$  in  $\mathcal{I}_k^*$  do
5       for  $j$  to  $J$  do
6          $\mathbf{x}_{i_k^*}^j \leftarrow \mathbf{x}_{i_k^*}^j \in \mathcal{D}_{i_k^*}$ 
7          $f(\mathbf{x}_{i_k^*}^j) \leftarrow \text{fun\_eval}(\mathbf{x}_{i_k^*}^j)$ 
8        $\mathcal{I}_k \leftarrow \text{partitioning}(\mathcal{D}_{i_k^*})$ 
9   return  $\min_{i_k \in \mathcal{I}_k} f(\mathbf{x}_{i_k})$ 
10 function selection( $\mathcal{I}_k$ )
11    $\mathcal{I}_k^* \leftarrow \mathcal{I}_k^* \subseteq \mathcal{I}_k$ 
12   return  $\mathcal{I}_k^*$ 
13 function partitioning( $\mathcal{D}_{i_k^*}$ )
14    $\mathcal{D}_{i_k^*} \leftarrow \bigcup_{j=1}^J \mathcal{D}_{i_k^*}^j$ 
15    $\mathcal{I}_k \leftarrow \mathcal{I}_k \cup \{|\mathcal{I}_k| + j\}_{j=1}^J$ 
16   return  $\mathcal{I}_k$ 
```

partitioning step.

The entire process described above is repeated until the termination criteria are met.

4.1 Selection

In the previous section, we presented a general partition scheme for Lipschitz optimization. Now, we dig into the algorithm's details by introducing the steps for estimating the local Lipschitz constants and selecting the partitions based on this information.

4.1.1 Adaptive Estimation of the Local Lipschitz Constants

In Lipschitz optimization, it is common practice to obtain information about the Lipschitz constant L and compute lower bounds of the objective function f to guide the algorithm towards regions where these bounds are lower. However, relying solely on the global Lipschitz constant estimates may not accurately reflect the behavior of the objective function in specific regions of the domain \mathcal{D} .

Consider a scenario where the objective function f is mostly flat, except for a small region within \mathcal{D} where it exhibits highly chaotic behavior (i.e., a higher Lipschitz constant). In such cases, the lower bounds computed around the gentler regions of \mathcal{D} would poorly estimate the true lower bounds because the global Lipschitz constant represents the overall maximum variation of f . Therefore, it is more informative to estimate the local Lipschitz constant \tilde{L}_i associated with each partition \mathcal{D}_i instead of relying entirely on the global Lipschitz constant L .

To introduce a local source of information about the function f when estimating the lower bounds, we consider the norm of the gradient at the centroid \mathbf{x}_i . However, to maintain the derivative-free nature of our procedure and to don't consume too many functions evaluations, we approximate the gradients around each centroid \mathbf{x}_i of the partitions \mathcal{D}_i using the points sampled thus far by the algorithm. This algorithmic choice has the effect that the accuracy of these gradient approximations directly depends on the size of each partition.

As the size of a partition \mathcal{D}_i decreases, the uncertainty about the behavior of the objective function around \mathcal{D}_i decreases as well. Therefore, it is reasonable to balance our estimate of the local Lipschitz constant \tilde{L}_i based on the size of its corresponding partition \mathcal{D}_i . To achieve this, we propose an adaptive formula

Definition 1. Given \mathcal{D}_{i_k} as a partition of the feasible space at iteration k , and let

$$\alpha_{i_k} = \frac{\|\mathbf{u}_{i_k} - \mathbf{l}_{i_k}\|}{\sqrt{N}}, \quad \alpha_{i_k} \in (0, 1), \quad \tilde{L}_k = \max_{i_k \in \mathcal{I}_k} \|\tilde{\nabla} f(\mathbf{x}_{i_k})\| \quad (4)$$

the estimation of the local Lipschitz constant L_{i_k} is given by

$$\tilde{L}_{i_k} = \alpha_{i_k} \tilde{L}_k + (1 - \alpha_{i_k}) \|\tilde{\nabla} f(\mathbf{x}_{i_k})\| \quad (5)$$

In Eq. 5, the term α_{i_k} is the ratio between the diagonal of the partition \mathcal{D}_{i_k} and the main diagonal of the feasible set \mathcal{D} (normalized to a unit hypercube). As the diagonal of the partition \mathcal{D}_{i_k} , denoted by $\|\mathbf{u}_{i_k} - \mathbf{l}_{i_k}\|$, decreases, the local information in the neighborhood of \mathcal{D}_{i_k} becomes more precise, and the estimate of the local Lipschitz constant is primarily influenced by the norm of the gradient approximation at \mathbf{x}_{i_k} , namely $\|\tilde{\nabla} f(\mathbf{x}_{i_k})\|$. On the other hand, if the diagonal of the partition \mathcal{D}_{i_k} is approximately equal to the maximum diagonal, the local information may not be reliable, and the estimate of the local Lipschitz constant relies more on the estimate of the global Lipschitz constant \tilde{L}_k , which represents the maximum absolute variation observed during the iterations of the algorithm.

In the following section, we define the criteria for selecting the partitions \mathcal{D}_{i_k} based on the information collected from our estimates of the local Lipschitz constants.

4.1.2 Selection Criteria

In the following definition, we show which partitions \mathcal{D}_{i_k} are selected in HALO.

Definition 2. Given the estimation of the local Lipschitz constant \tilde{L}_{i_k} for every $i_k \in \mathcal{I}_k$ from Eq. 5, then the partition \mathcal{D}_{i_k} is selected if at least one of the following conditions is satisfied

Criterion 1 if for $i_k \in \mathcal{I}_k$, then

$$f(\mathbf{x}_{i_k}) - \tilde{L}_{i_k} \frac{\|\mathbf{u}_{i_k} - \mathbf{l}_{i_k}\|}{2} \leq f(\mathbf{x}_{j_k}) - \tilde{L}_{j_k} \frac{\|\mathbf{u}_{j_k} - \mathbf{l}_{j_k}\|}{2} \quad \forall j \in \mathcal{I}_k \quad (6)$$

Criterion 2 For $i_k \in \mathcal{I}_k$, then

$$f(\mathbf{x}_{i_k}) = f_{\min} \quad (7)$$

where $f_{\min} = \min_{j_k \in \mathcal{I}_k} f(\mathbf{x}_{j_k})$

Criterion 3 if for $i_k \in \mathcal{I}_k^{max}$ and

$$f(\mathbf{x}_{i_k}) - \tilde{L}_{i_k} \frac{\|\mathbf{u}_{i_k} - \mathbf{l}_{i_k}\|}{2} \leq f(\mathbf{x}_{j_k}) - \tilde{L}_{j_k} \frac{\|\mathbf{u}_{j_k} - \mathbf{l}_{j_k}\|}{2} \quad \forall j \in \mathcal{I}_k^{max} \quad (8)$$

$$\text{where } \mathcal{I}_k^{max} = \{i_k \in \mathcal{I}_k : \frac{\|\mathbf{u}_{i_k} - \mathbf{l}_{i_k}\|}{2} = \max_{i_k \in \mathcal{I}_k} \frac{\|\mathbf{u}_{i_k} - \mathbf{l}_{i_k}\|}{2}\}.$$

The selection criteria defined in Def. 2 determine which partitions \mathcal{D}_{i_k} are selected in the HALO algorithm. Let's examine each criterion

- **Criterion 1:** This criterion selects the partition \mathcal{D}_{i_k} that achieves the lowest lower bound, considering the information collected from the local Lipschitz constants. The lower bound is computed as $f(\mathbf{x}_{i_k}) - \tilde{L}_{i_k} \|\mathbf{u}_{i_k} - \mathbf{l}_{i_k}\|/2$, where $f(\mathbf{x}_{i_k})$ is the function value at the centroid of \mathcal{D}_{i_k} , \tilde{L}_{i_k} is the estimated local Lipschitz constant, and $\|\mathbf{u}_{i_k} - \mathbf{l}_{i_k}\|/2$ is the distance from the center to the vertices of the partition. This criterion aims to select partitions that provide the most promising lower bounds based on the local behavior of the objective function.
- **Criterion 2:** This criterion ensures that the partition with the lowest function value, denoted as f_{\min} , is always selected. This condition is beneficial when HALO is used in high-dimensional spaces and in a limited number of function evaluation scenarios, allowing the algorithm to obtain a decent reduction in the objective function value in a few iterations.
- **Criterion 3:** Among the partitions with the maximum diagonal size, which are denoted as \mathcal{I}_k^{max} , this criterion selects the partition that achieves the lowest lower bound. The lower bound is computed similarly as in Criterion 1. This criterion is significant for the convergence of the algorithm, as we will see in the following sections.

In Fig. 1, we can compare the selection criteria of HALO with those of the DIRECT algorithm, specifically targeting the potentially optimal partitions. We used the synthetic function generator presented in [40] for this particular example. Notably, HALO follows distinct trajectories from DIRECT, as none of its selected partitions align with the potentially optimal rectangles. In fact, HALO has the ability to choose rectangles that can be arbitrarily distant from the potentially optimal partitions of DIRECT. This allows HALO to proactively explore interesting partitions by leveraging its knowledge of the local Lipschitz constants. As illustrated in Fig. 1, HALO efficiently identifies the partition (indicated by the white star) where the global minimum is located since is the one that satisfies Criterion 1, while DIRECT experiences a delay in identifying the optimal partition.

4.2 Partitioning

In this section, we discuss the geometric properties of the feasible set \mathcal{D} and its partitioning, as well as the adaptive approximation of derivatives around each partition during the iterations.

4.2.1 Division and Sampling

During the global search carried out by HALO, we employ the same sampling and division criteria as the DIRECT algorithm [18]. This choice was made due to the

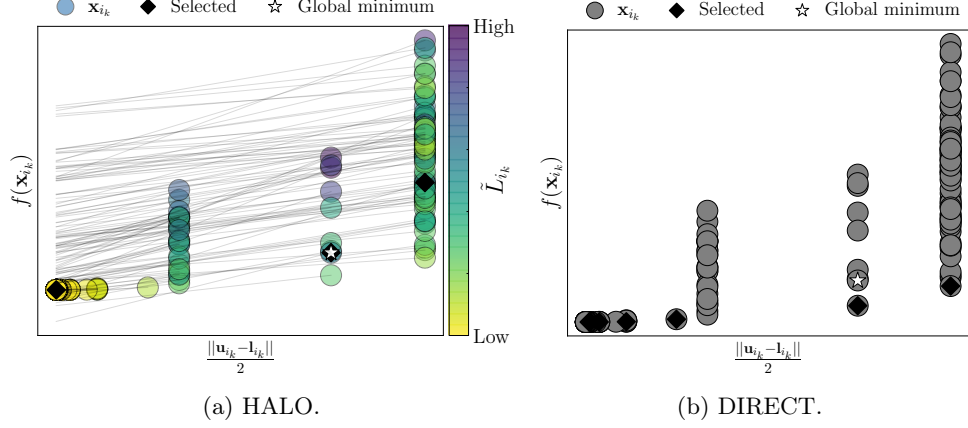


Fig. 1: Comparison between the selection criteria of HALO (Fig. 1a) and the potentially optimal selection criteria of DIRECT (Fig. 1b). The x -axis represents the distance from the center to the vertices of each partition, while the y -axis represents the corresponding function values. In Fig. 1a, the colormap indicates the values of the local Lipschitz constants \tilde{L}_{i_k} . The gray lines in Fig. 1a emphasize the lower bound values obtained at the vertices, with their slope determined by \tilde{L}_{i_k} . The selected partitions and the location of the global minimum are denoted by black rhombuses and a white star respectively.

robustness and relative simplicity of the DIRECT algorithm, making it easier to understand and implement the code.

Let's describe how the partitions \mathcal{D}_{i_k} are generated in the DIRECT algorithm. We define the vector $\mathbf{s}_{i_k} \in \mathbb{R}^N$ associated with the partition \mathcal{D}_{i_k} which measures the distance from its centroid to its boundary along each coordinate direction. Specifically, \mathbf{s}_{i_k} represents half the length of the sides of the partition at iteration k

$$\mathbf{s}_{i_k} = [|u_{i_k}^n - l_{i_k}^n|/2]_{n=0}^N \quad (9)$$

we define the set of indices \mathcal{P}_{i_k} that contains the n th coordinate directions where the partition \mathcal{D}_{i_k} has its longest side

$$\mathcal{P}_{i_k} = \{n \in \mathbb{N} : s_{i_k}^{max} = \max\{s_{i_k}^n\}_{n=0}^N\} \quad (10)$$

Subsequently, two points $\mathbf{x}_{i_k}^{p1}$ and $\mathbf{x}_{i_k}^{p2}$ are sampled for each coordinate axis parallel to the longest side of \mathcal{D}_{i_k} (namely along the p th coordinate)

$$\mathbf{x}_{i_k}^{p1} = \mathbf{x}_{i_k} + \Delta_{i_k} \mathbf{e}_p, \quad \mathbf{x}_{i_k}^{p2} = \mathbf{x}_{i_k} - \Delta_{i_k} \mathbf{e}_p, \quad \forall p \in \mathcal{P}_{i_k} \quad (11)$$

here, \mathbf{e}_p represents the p th orthonormal base of \mathbb{R}^N and the scalar Δ_{i_k} is given by two third the longest side of \mathcal{D}_{i_k}

$$\Delta_{i_k} = \frac{2}{3} s_{i_k}^{max} \quad (12)$$

From Eq. 11 is evident that two new points are generated along the coordinate of the longest side of the selected partition, resulting in a total of $J = 2|\mathcal{P}_{i_k}|$ new points generated per selected partition.

Once the sampling within a selected partition \mathcal{D}_{i_k} is complete, we proceed with the division. In the DIRECT algorithm, the idea is to divide a partition into hypercubes and hyperrectangles, ensuring that the partition with the lowest objective function value always has the longest diagonal.

We define the set \mathcal{T}_{i_k} which collects the minimum objective function value among the two newly generated points $\mathbf{x}_{i_k}^{p_1}$ and $\mathbf{x}_{i_k}^{p_2}$ for each coordinate axis parallel to the longest side of \mathcal{D}_{i_k}

$$\mathcal{T}_{i_k} = \mathcal{T}_{i_k} \cup \{\min\{f(\mathbf{x}_{i_k}^{p_1}), f(\mathbf{x}_{i_k}^{p_2})\}\}, \quad \forall p \in \mathcal{P}_{i_k} \quad (13)$$

we proceed to divide \mathcal{D}_{i_k} in the order given by \mathcal{T}_{i_k} and perpendicular to the direction \mathbf{e}_p such that all the p th sides of \mathbf{s}_{i_k} are reduced by half of Δ_{i_k} (or equivalently by a third the longest side of the partition \mathcal{D}_{i_k})

$$s_{i_k}^p = \frac{1}{2}\Delta_{i_k} = \frac{1}{3}s_{i_k}^{max}, \quad s_{i_k}^{p_1} = s_{i_k}^{p_2} = s_{i_k}^p \quad \forall p \in \mathcal{P}_{i_k} \quad (14)$$

Additionally, the sides $s_{i_k}^{p_1}$ and $s_{i_k}^{p_2}$ of the two new partitions are updated accordingly.

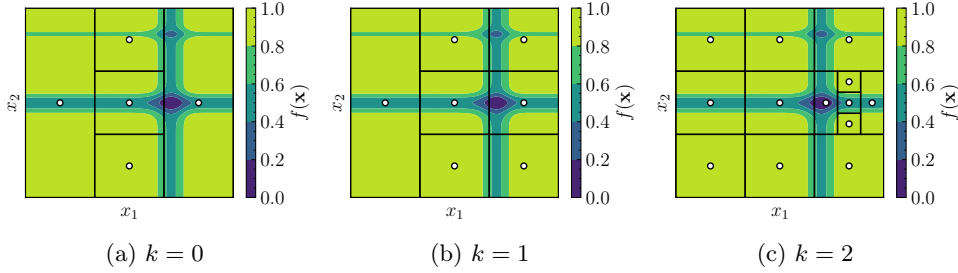


Fig. 2: A graphical representation of the division and sampling step. White dotted points the centroids \mathbf{x}_{i_k} , in red we highlight the boundaries of the partitions. The colorbar shows normalized function values.

4.2.2 Adaptive Gradients Approximation

In this section we describe how the vector $\tilde{\nabla}f(\mathbf{x}_{i_k})$ from Eq. 5 is computed. After the sampling and division processes, the algorithm collects information about the behavior of the objective function around each partition. To achieve this, a vector is associated with each partition, which describes the intensity of variation of the objective function inside that partition in terms of absolute slopes. This vector adaptively collects the absolute slopes along each coordinate computed based on the points generated so far by the algorithm. We define the nearest neighbors of a partition \mathcal{D}_{i_k} as the indices of the nearest points along each coordinate axis.

Definition 3. Given the partition \mathcal{D}_{i_k} and its centroid \mathbf{x}_{i_k} we define the nearest neighbors of \mathbf{x}_{i_k} the set of indices \mathcal{N}_{i_k} which contains the indices of the nearest points along the coordinate axis of \mathbb{R}^N .

The following property is satisfied by the current partition scheme

Property 1. Given the representative point \mathbf{x}_{i_k} which is center of its relative partition \mathcal{D}_{i_k} . Then if for every iteration $k > \bar{k}$, the partition \mathcal{D}_{i_k} is selected, the nearest neighbours of \mathbf{x}_{i_k} are given by

$$\mathbf{x}_{i_k} \pm \Delta_{i_k} \mathbf{e}_n \in \mathcal{N}_{i_k}, \quad n = 1, \dots, N \quad (15)$$

where \mathbf{e}_n is the n th orthonormal basis of \mathbb{R}^N and \mathcal{N}_{i_k} the set of the nearest neighbours of \mathbf{x}_{i_k} .

The nearest neighbors of a partition \mathcal{D}_{i_k} are defined as the indices of the nearest points along each coordinate axis. If the partition \mathcal{D}_{i_k} is always selected after a certain iteration \bar{k} , the nearest neighbors of its centroid \mathbf{x}_{i_k} are located at distances $\pm \Delta_{i_k}$ along each coordinate axis.

If a selected partition \mathcal{D}_{i_k} is a hypercube, it generates $J = 2N$ nearest points along all N coordinate axes. In this case, we compute the absolute slope at the centroid \mathbf{x}_{i_k} using a central difference formula

$$|\tilde{\nabla} f(\mathbf{x}_{i_k})_n| = \frac{|f(\mathbf{x}_{i_k}^{p_1}) - f(\mathbf{x}_{i_k}^{p_2})|}{2\Delta_{i_k}}, \quad n = 1, \dots, N \quad (16)$$

Here, $\mathbf{x}_{i_k}^{p_1}$ and $\mathbf{x}_{i_k}^{p_2}$ are the two points generated from the centroid \mathbf{x}_{i_k} along the n th coordinate axis. Similarly, we need to compute the slopes for the new points $\mathbf{x}_{i_k}^j$ generated by the partition \mathcal{D}_{i_k} at iteration k . The approximation of the gradient associated with $\mathcal{D}_{i_k}^j$ is given by

$$|\tilde{\nabla} f(\mathbf{x}_{i_k}^j)_n| = \begin{cases} \frac{|f(\mathbf{x}_{i_k}^j) - f(\mathbf{x}_{i_k})|}{\Delta_{i_k}}, & \text{if } \mathbf{x}_{i_k} \in \mathcal{N}_{i_k}^j. \\ |\tilde{\nabla} f(\mathbf{x}_{i_k})_n|, & \text{otherwise.} \end{cases} \quad (17)$$

For the remaining $N - 1$ coordinates, the absolute slopes $|\tilde{\nabla} f(\mathbf{x}_{i_k}^j)_n|$ are set to the slope of \mathbf{x}_{i_k} . Although this approach may lead to an incorrect estimation of the gradient associated with the partition $\mathcal{D}_{i_k}^j$, the effect is negligible as either the partition $\mathcal{D}_{i_k}^j$ will be selected and its gradient updated or the size of the partition $\mathcal{D}_{i_k}^j$ is already relatively small.

If the selected partition \mathcal{D}_{i_k} is a hyperrectangle, it generates $J = 2|\mathcal{P}_{i_k}|$ nearest points along all $|\mathcal{P}_{i_k}|$ coordinate axes. The absolute slope is calculated using the same central difference formula as before

$$|\tilde{\nabla} f(\mathbf{x}_{i_k})_n| = \begin{cases} \frac{|f(\mathbf{x}_{i_k}^{p_1}) - f(\mathbf{x}_{i_k}^{p_2})|}{2\Delta_{i_k}}, & \text{if } \mathbf{x}_{i_k}^{p_1}, \mathbf{x}_{i_k}^{p_2} \in \mathcal{N}_{i_k}. \\ |\tilde{\nabla} f(\mathbf{x}_{i_k})_n|, & \text{otherwise.} \end{cases} \quad (18)$$

For the remaining $N - |\mathcal{P}_{i_k}|$ coordinates we leave the slope unchanged in those directions. As shown previously we also update the slopes for the points that \mathcal{D}_{i_k} has generated.

In this case, the procedure is the same as in the case if the partition \mathcal{D}_{i_k} is a hypercube when selected.

The simple procedure described above tries to adaptively update the absolute slopes at each selected centroid and at its neighbors only using the points sampled so far by the algorithm.

4.3 Coupling Strategy with Local Optimization Methods

In this work, we propose to integrate our approach with local optimizers to improve its convergence speed. The reason behind this is that the sampling scheme used in the DIRECT algorithm, as described in section 4.2.1, can be inefficient when the algorithm approaches a stationary point. The rigid structure of the sampling scheme, where the algorithm is forced to sample along predefined coordinate directions with constant step sizes, can slow down the convergence of the HALO algorithm.

To address this issue, we introduce a coupling strategy that incorporates local optimization routines only when a point is likely to be in the vicinity of a stationary point, to avoid overusing them. The strategy is as follows: if the selected partition satisfies either [Criterion 1](#) or [Criterion 2](#) (or both) in Def. 2, and if the half diagonal of the partition is less than a scalar β then the centroid of the partition is considered as a starting point for the local optimizer

$$\frac{\|\mathbf{u}_{i_k} - \mathbf{l}_{i_k}\|}{2} \leq \beta \quad (19)$$

To ensure that the local optimizer doesn't start from a similar location in the domain, we perform a nearest-neighbor search. Before starting the local optimization from the centroid, we identify all the points within a ball centered at the centroid with radius r . These points are saved in a set called \mathcal{C}_k , which includes the indices j of the neighboring points. The set \mathcal{C}_k is defined as follows

$$\mathcal{C}_k = \{j_k : \|\mathbf{x}_{i_k} - \mathbf{x}_{j_k}\| \leq r\}, \quad \forall j_k \in I_k, \quad i_k \neq j_k \quad (20)$$

Then, the local optimizer starts from the centroid \mathbf{x}_{i_k} with the updated set of indices

$$\mathcal{C}_k \cup i_k \quad (21)$$

If a new candidate point \mathbf{x}_{p_k} satisfies either condition [Criterion 1](#) or [Criterion 2](#) (or both), and the corresponding partition \mathcal{D}_{p_k} satisfies Eq. 19, the local search starts from \mathbf{x}_{p_k} only if the set \mathcal{B}_k is empty. The set \mathcal{B}_k is defined as

$$\mathcal{B}_k = \{j_k : \|\mathbf{x}_{p_k} - \mathbf{x}_{j_k}\| \leq r\}, \quad \forall j_k \in \mathcal{C}_k \quad (22)$$

If \mathcal{B}_k is empty, indicating that \mathbf{x}_{p_k} is not close to any neighbors already collected in \mathcal{C}_k , the local optimizer starts from \mathbf{x}_{p_k} and the set \mathcal{C}_k is updated with the neighbors of p_k

$$\mathcal{C}_k = \mathcal{C}_k \cup \{j_k : \|\mathbf{x}_{p_k} - \mathbf{x}_{j_k}\| \leq r\}, \quad \forall j_k \in I_k, \quad p_k \neq j_k \quad (23)$$

Then, the local optimizer is initiated from \mathbf{x}_{p_k} and the set \mathcal{C}_k is updated with p_k . On the other hand, if \mathcal{B}_k is not empty, indicating that \mathbf{x}_{p_k} is close to some neighbors in \mathcal{C}_k , the local search does not start from \mathbf{x}_{p_k} . The set \mathcal{C}_k is still updated with p_k

$$\mathcal{C}_k \cup p_k \quad (24)$$

In this case, the partition \mathcal{D}_{p_k} is not sampled or divided, and the radius r should be set to a relatively small value, such as $r = 10^{-4}$, to avoid excluding large portions of the domain.

4.4 Convergence and Stopping Criteria

In this paragraph, we will discuss the convergence properties of the HALO algorithm. First, we introduce a property that characterizes the partitions generated during the iterations

Property 2. *The sequence of partitions $\{\mathcal{D}^{i_k}\}$ is strictly nested if and only if*

$$\bigcap_{k=0}^{+\infty} \mathcal{D}_{i_k} = \mathbf{x}_{i_k} \quad (25)$$

or equivalently that

$$\lim_{k \rightarrow +\infty} \|\mathbf{u}_{i_k} - \mathbf{l}_{i_k}\| = 0 \quad (26)$$

Property 2 states that when a partition \mathcal{D}_{i_k} is continuously selected and divided, it collapses to \mathbf{x}_{i_k} .

According to [13], for the HALO algorithm to converge to a global minimum, the sequence of points generated by the algorithm must be dense in \mathcal{D} . We can establish a proposition that shows how the everywhere dense property of HALO is achieved when the largest partitions are always selected

Proposition 1. *Given that Property 2 is satisfied, if for every iteration k the largest partitions \mathcal{D}_{i_k} is always selected such that $i_k \in \mathcal{I}_k^{\max}$, then for $k \rightarrow \infty$ and for every $\tilde{\mathbf{x}} \in \mathcal{D}$, the sequence of sets $\{\mathcal{D}_{i_k}\}$ are dense such that*

$$\bigcap_{k=0}^{\infty} \mathcal{D}_{i_k} = \{\tilde{\mathbf{x}}\} \quad \forall i_k \in \mathcal{I}_k \quad (27)$$

Proof. The proof follows from the fact that the following identity holds for every i_k and that Criterion 3 is always met

$$\lim_{k \rightarrow +\infty} \|\mathbf{u}_{i_k} - \mathbf{l}_{i_k}\| \leq \|\mathbf{u}_{j_k} - \mathbf{l}_{j_k}\| = 0 \quad (28)$$

with $j_k \in \mathcal{I}_k^{\max}$, with $\mathcal{I}_k^{\max} = \{i_k \in \mathcal{I}_k : \|\mathbf{u}_{i_k} - \mathbf{l}_{i_k}\| = \max_{i_k \in \mathcal{I}_k} \|\mathbf{u}_{i_k} - \mathbf{l}_{i_k}\|\}$. \square

Therefore, if the algorithm produces dense sets across all the domain \mathcal{D} , then for k sufficiently large the algorithm will converge also at the global minimum of f .

Generally, rather than producing an everywhere dense set we often aim for an algorithm that produces denseness primarily around the global minimizers and not throughout the entire domain \mathcal{D} . However, achieving this in practice is very difficult, especially without prior knowledge of the global Lipschitz constant [42]. Hence, the stopping criterion for HALO is mainly based on the maximum number of function evaluations, which is a commonly used criterion in engineering applications.

However, we can show that the exact value of the global Lipschitz constant can be obtained when the algorithm iterates indefinitely to infinity. First, we can highlight an important characteristic of the distance Δ_{i_k} in the next proposition

Proposition 2. *Given the center \mathbf{x}_{i_k} of its relative partition \mathcal{D}_{i_k} . If the algorithm satisfies Property 2 and Property 1 then the distance Δ_{i_k} from the nearest point of \mathbf{x}_{i_k} satisfies the following limit*

$$\lim_{k \rightarrow +\infty} \Delta_{i_k} = 0 \quad (29)$$

Proof. If Property 2 holds the algorithm produces at least one sequence of strictly nested partitions $\{\mathcal{D}^{i_k}\}$ such that

$$\lim_{k \rightarrow +\infty} \|\mathbf{u}_{i_k} - \mathbf{l}_{i_k}\| = 0 \quad (30)$$

then we know that if the partition \mathcal{D}_{i_k} is selected, then exactly $J = 2|\mathcal{P}_{i_k}|$ (see Eq. 10) points are sampled inside \mathcal{D}_{i_k} . Consequently given Property 1, for every $j = 1, \dots, J$ we have that

$$\Delta_{i_k} = \|\mathbf{x}_{i_k} - \mathbf{x}_{i_k}^j\| \leq \|\mathbf{u}_{i_k} - \mathbf{l}_{i_k}\| \quad (31)$$

considering Eq. 30 it follows that $\lim_{k \rightarrow +\infty} \Delta_{i_k} = 0$ \square

Proposition 2 states that the minimum distance Δ_{i_k} from the nearest point to \mathbf{x}_{i_k} tends to zero as the iteration k approaches infinity and as the partition \mathcal{D}_{i_k} is continuously selected. Thus, as a partition \mathcal{D}_{i_k} is selected during the iterations, the information contained in the vector $\tilde{\nabla}f(\mathbf{x}_{i_k})$ becomes more precise, so that we can introduce the following propositions

Proposition 3. *Given the representative point \mathbf{x}_{i_k} which is center of its relative partition \mathcal{D}_{i_k} . If HALO satisfies has Property 2 and Property 1 then the vector $\tilde{\nabla}f(\mathbf{x}_{i_k})$ associated to the partition \mathcal{D}_{i_k} converge to the true gradient at \mathbf{x}_{i_k}*

$$\lim_{k \rightarrow +\infty} \tilde{\nabla}f(\mathbf{x}_{i_k}) = \nabla f(\mathbf{x}_{i_k}) \quad (32)$$

Proof. If Property 1 is satisfied then there exist k such that for every $\bar{k} > k$ the centroid \mathbf{x}_{i_k} has its nearest point along all the coordinate directions. Then using the results from Property 2 and for the definition of derivative it follows that $\lim_{k \rightarrow +\infty} \tilde{\nabla}f(\mathbf{x}_{i_k}) = \nabla f(\mathbf{x}_{i_k})$. \square

Proposition 4. *If HALO satisfies Proposition 3 then*

$$\lim_{k \rightarrow \infty} \max_{i_k \in \mathcal{I}_k} \{\|\tilde{\nabla}f(\mathbf{x}_{i_k})\|\} = L \quad (33)$$

Proof. The proof is given directly by using the results of Proposition 3 and applying it for every $i_k \in \mathcal{I}_k$ and taking the maximum. \square

Proposition 3 further shows that as the selected partition becomes denser the associated vector $\tilde{\nabla}f(\mathbf{x}_{i_k})$ becomes a more accurate approximation of the true gradient $\nabla f(\mathbf{x}_{i_k})$. As a result, from Proposition 4 the global Lipschitz constant L can be accurately estimated.

4.5 A Detailed Implementation of HALO

The simplified pseudocode of HALO is presented in Algorithm 2. In the following, we will describe the main steps of the pseudocode. The core part of HALO resides within the **Main** function, which takes as input the termination criterion for the algorithm, either based on the maximum number of function evaluations or the maximum number of iterations. The user also provides the box constraints of the optimization problem \mathcal{D} .

Starting with the counter k set to zero, lines 9 and 10 define the indices of the selected partitions \mathcal{I}_k^* and the matrix $\mathbf{S} \in \mathbb{R}^{|\mathcal{I}_k^*| \times N}$, where each entry contains the vector \mathbf{s} defined in Eq. 9. In line 11, a for loop begins, iterating over the indices of each selected partition. This loop is primarily responsible for computing $\Delta_{i_k^*}$ as described in Section 4.2.1. In line 17, another for loop starts, cycling through each element of the set $\mathcal{P}_{i_k^*}$ defined in line 14 and Eq. 10. This loop handles the sampling process described in Section 4.2.1. Additionally, we compute the slopes by updating the matrix $\mathbf{G} \in \mathbb{R}^{|\mathcal{I}_k^*| \times N}$, which stores the gradient estimations discussed in Section 4.2.2. The notation $\mathbf{G}_{i_k^*, p}$ indicates that the p th coordinate of the gradient relative to the i_k^* th partition is being updated. After this inner for loop, line 28 performs a sorting of the indices of the set $\mathcal{T}_{i_k^*}$ defined in Eq. 13, and line 29 calls the function (line 68) responsible for dividing the set $\mathcal{D}_{i_k^*}$.

Once the outer loop defined in line 11 is completed, based on the information in the matrix \mathbf{G} , we invoke the function that computes the values of the local Lipschitz constants, stored in the vector $\mathbf{l} \in \mathbb{R}^{|\mathcal{I}_k^*|}$. Lines 31 and 32 define the vectors $\mathbf{v} \in \mathbb{R}^{|\mathcal{I}_k^*|}$ and $\mathbf{h} \in \mathbb{R}^{|\mathcal{I}_k^*|}$, which contain half of the distances from the center of each partition j to its vertices and the norm of each gradient estimation (i.e., the norm of each row of \mathbf{G}). Line 34 computes the estimation of the local Lipschitz constant in a vectorized form, following Eq. 5.

The next task is to use the local Lipschitz constants collected in the vector \mathbf{l} to compute the lower bounds and select the most promising partitions based on Def. 2. The lower bound values are stored in the vector $\mathbf{r} \in \mathbb{R}^{|\mathcal{I}_k^*|}$ (line 37). The indices q_1^* , q_2^* , and q_3^* represent the index of the partition with the minimum lower bound (Criterion 1), the partition with the minimum objective function value (Criterion 2), and the partition with the largest diagonal that has the minimum lower bound (Criterion 3). It is possible for one index to satisfy multiple conditions (e.g., $q_1^* = q_2^*$), so care should be taken to avoid duplicate entries in the set \mathcal{I}_k^* . In lines 42 and 47, we check if a local search has already been performed from the centroid of a partition and if it satisfies Eq. 19. If both conditions are met, the local search is initiated as explained in Section 4.3. Note that the largest hyperrectangle q_3^* is always selected (line 52). Finally, the set of selected partitions is returned, and a new loop can begin, iterating over its elements.

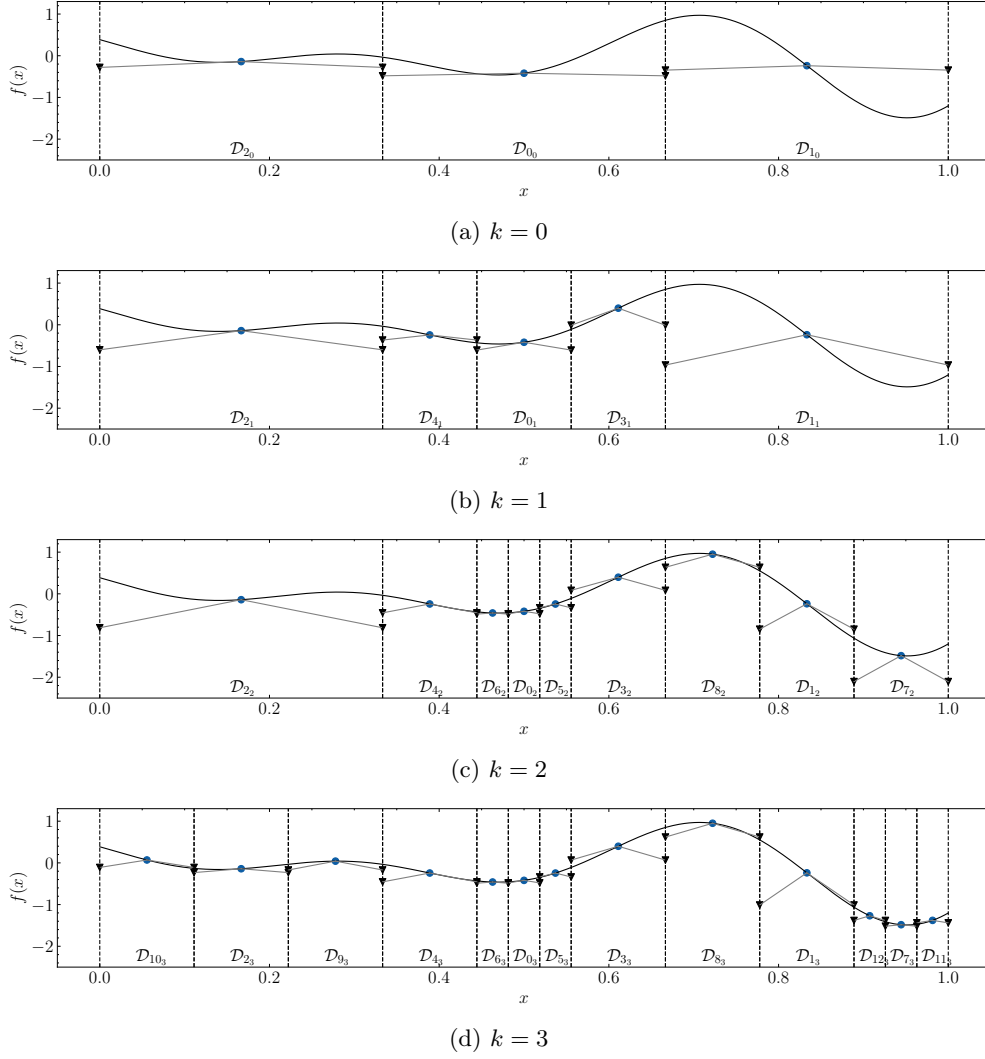


Fig. 3: An example of HALO for a one-dimensional function. The blue rounded dots represent the centroids of each partition, the grey lines highlight the slope of the local Lipschitz constant, and the black triangles indicate the lower bound values at the boundaries of each partition.

To conclude this section, Fig. 3 illustrates the behavior of HALO for a simple one-dimensional function. At iteration $k = 0$, it can be observed that the values of the Lipschitz constants for the three partitions do not reflect the underlying trend of the objective function because these three points have similar objective function values, and there is a relatively large distance between them. At iteration $k = 1$, only the partition \mathcal{D}_0 is selected and divided because it satisfies [Criterion 1](#), [Criterion 2](#), and [Criterion](#)

3. The lower bound values are already more precise at this stage. At iteration $k = 2$, two intervals are selected and divided: \mathcal{D}_0 , which satisfies [Criterion 2](#) (has the lowest function value), and \mathcal{D}_1 , which satisfies [Criterion 1](#) and [Criterion 3](#) (it has the lowest overall lower bound and is the largest partition with the lowest lower bound). Finally, at iteration $k = 3$, two more intervals are divided: \mathcal{D}_2 , which satisfies [Criterion 3](#), and \mathcal{D}_7 , which satisfies [Criterion 1](#) and [Criterion 2](#). The last figure (Fig. 3d), demonstrates that all the lower bound values are now quite precise. This entire process is automated in HALO, requiring no critical hyperparameters to be set by the user.

5 Numerical Results

In this section, we conduct a comprehensive evaluation of the HALO algorithm compared to other GO algorithms. The evaluation is performed on a diverse set of test functions organized into three different benchmarks. Additionally, we conduct a parametric study on the parameter β from Eq. 19 to provide general recommendations to users regarding its value. Finally, we show how to extract insightful information from the objective function using our approach.

The code for the algorithms and test functions used in this study can be found in the following GitHub repository <https://github.com/dannyzx/HALO>.

5.1 Experimental Setup

In the following paragraphs, we provide details about the algorithms, test functions, and stopping criteria used in our numerical experiments.

5.1.1 Algorithms

The following algorithms are included in our numerical experiments:

- HALO_{L-BFGS-B} and HALO_{SDBOX}: These are two versions of HALO that are coupled with different local optimizers. HALO_{L-BFGS-B} utilizes a quasi-Newton method for bound-constrained problems (L-BFGS-B) [37], while HALO_{SDBOX} uses a derivative-free coordinate descent method with an Armijo-type linesearch for bound-constrained optimization [38] (SD-BOX). Both versions of HALO have a single hyperparameter, β , which is defined in Eq. 19. This parameter determines the minimum size a selected partition must have before a local search can be initiated from its centroid. For our experiments, we fix β to 10^{-4} . In HALO_{L-BFGS-B}, the gradients used in the Quasi-Newton code are computed using finite difference methods.
- HLO: This is similar to HALO_{SDBOX}, but it does not use adaptive estimates of the local Lipschitz constants as defined in Eq. 5. Instead, the lower bounds are calculated based on the estimate of the global Lipschitz constant only. In other words, all local Lipschitz constants are fixed as $\tilde{L}_{i_k} = \max_{i_k \in \mathcal{I}_k} \|\tilde{\nabla} f(\mathbf{x}_{i_k})\|$. This allows us to compare the convergence acceleration achieved by estimating the local Lipschitz constants with using only the estimate of the global Lipschitz constant.

Algorithm 2: Hybrid Adaptive Lipschitzian Optimization (HALO)

```

1 function Main(max_iter, max_fun_eval, D)
2   k ← 0
3   C_k, G, S, f ← ∅, [[ ]], [[ ]], [ ]
4   for k to max_iter do
5     if k > 0 then
6       l ← compute_Lipschitz(G, S)
7       T_k^* ← selection(I_k, l, C_k)
8     else
9       T_k^* ← {0}
10      S_{i_k} ← [|u_n - l_n|/2]_{n=1}^N
11      for i_k^* in I_k^* do
12        s_{i_k^*}^* ← S_{i_k^*}^*
13        s_{i_k^*}^{max} ← max{s_{i_k^*}^*}
14        P_{i_k^*}^* ← arg max{s_{i_k^*}^*}
15        Δ_{i_k^*}^* ←  $\frac{2}{3} s_{i_k^*}^{max}$ 
16        V_{i_k^*}^* ← ∅
17        for p in P_{i_k^*}^* do
18          x_{i_k^*}^{p1} ← x_{i_k^*}^* + Δ_{i_k^*}^* e_p
19          f(x_{i_k^*}^{p1}) ← fun_eval(x_{i_k^*}^{p1})
20          f_{i_k^*+1}^* ← f(x_{i_k^*}^{p1})
21          G_{i_k^*+1,p}^* ← |f(x_{i_k^*}^{p1}) - f(x_{i_k^*}^*)|/Δ_{i_k^*}^*
22          x_{i_k^*}^{p2} ← x_{i_k^*}^* - Δ_{i_k^*}^* e_p
23          f(x_{i_k^*}^{p2}) ← fun_eval(x_{i_k^*}^{p2})
24          f_{i_k^*+2}^* ← f(x_{i_k^*}^{p2})
25          G_{i_k^*+2,p}^* ← |f(x_{i_k^*}^{p2}) - f(x_{i_k^*}^*)|/Δ_{i_k^*}^*
26          G_{i_k^*+p}^* ← |f(x_{i_k^*}^{p1}) - f(x_{i_k^*}^{p2})|/2Δ_{i_k^*}^*
27          T_{i_k^*}^* ← T_{i_k^*}^* ∪ {min{f(x_{i_k^*}^{p1}), f(x_{i_k^*}^{p2})}}
28        U_{i_k^*}^* ← arg sort{T_{i_k^*}^*}
29      I_k ← partitioning(U_{i_k^*}^*, S, V)
30 function compute_local_Lipschitz(G)
31   v ← (||S_j||)_{1 ≤ j ≤ |I_k|}
32   h ← (||G_j||)_{1 ≤ j ≤ |I_k|}
33   α ← v/√N
34   l ← α ⊙ h + (1 - α) ⊙ max{h}
35   return l
36 function selection(I_k, C_k)
37   r ← f - v ⊙ l
38   q_1^* ← arg min{r}
39   q_2^* ← arg min{f}
40   Q_3 ← arg max{v}
41   q_3^* = arg min_{q_3 ∈ Q_3} {1}
42   if q_1^* ∉ C_k and v_{q_1^*} ≤ β then
43     x^0 ← x_{q_1^*}
44     local_search(x_{q_1^*}, C_k)
45   else
46     I_k^* ← I_k^* ∪ {q_1^*}
47   if q_2^* ∉ C_k and v_{q_2^*} ≤ β then
48     x^0 ← x_{i_k^*}
49     local_search(x_{q_2^*}, C_k)
50   else
51     I_k^* ← I_k^* ∪ {q_2^*}
52   I_k^* ← I_k^* ∪ {q_3^*}
53   return I_k^*
54 function local_search(x^0, C_k)
55   x_{p_k} ← x^0
56   if C_k = ∅ then
57     C_k ← {j ∈ I_k : ||x_{p_k} - x_{j_k}|| ≤ r}
58     x ← local_optimizer(x_{p_k})
59     return x
60   else
61     B_k ← {j ∈ C_k : ||x_{p_k} - x_{j_k}|| ≤ r}
62     if B_k ≠ ∅ then
63       C_k ← C_k ∪ {j ∈ I_k : ||x_{p_k} - x_{j_k}|| ≤ r}
64       x ← local_optimizer(x_{p_k})
65       return x
66     else
67       C_k ← C_k ∪ p_k
68 function partitioning(U_{i_k^*}^*, P_{i_k^*}^*, S, V)
69   for u in U_{i_k^*}^* do
70     m ← P_{i_k^*}^*, u
71     S_{i_k^*+m}^* ← Δ/2
72     S_{i_k^*+1}^* ← S_{i_k^*}^*
73     S_{i_k^*+2}^* ← S_{i_k^*}^*
74     I_k ← I_k ∪ {|I_k| + 1, |I_k| + 2}
75   return I_k

```

- DIRECT [18]: This is the classical DIRECT algorithm, with a fixed hyperparameter ϵ set to $10^{-4}|f_{\min}|$, as suggested in [18].
- DIRMIN [36]: it is an efficient hybridization of the DIRECT algorithm. It starts local optimizations from each of the potentially optimal hyperrectangles identified by DIRECT. We use the same derivative-free local optimizer as in HALO_{SDBOX}, which is the algorithm defined in [38]. DIRMIN has shown improved convergence compared to DIRECT on various test functions [36], and it outperformed other derivative-free hybrid GO algorithms in a real-world hull form shape optimization problem [43].
- CMA-ES [5]: it is a popular stochastic meta-heuristic approach known for its strong performance in various applications. It is considered one of the most competitive algorithms in its category [44]. We fix the hyperparameter σ_0 to be 1/4 of the domain, as recommended by the author. Due to the stochastic nature of the algorithm, we run 50 independent experiments for each test function.

5.1.2 Test Functions

We conducted our algorithm evaluations using three distinct benchmarks. Here are the details of each benchmark:

1. First Benchmark: it is constructed using a function generator described in [40]. We considered 100 test functions for each dimension N ranging in $\{2, 3, 4, 6, 8, 10\}$, resulting in a total of 600 different test functions. The function generator requires two hyperparameters: the number of stationary points and their smoothness. For this experiment, we uniformly sampled the number of stationary points S from the range 1 to 100, and the smoothness parameter was chosen uniformly from the range $[2, 3]$, following the approach in [45].

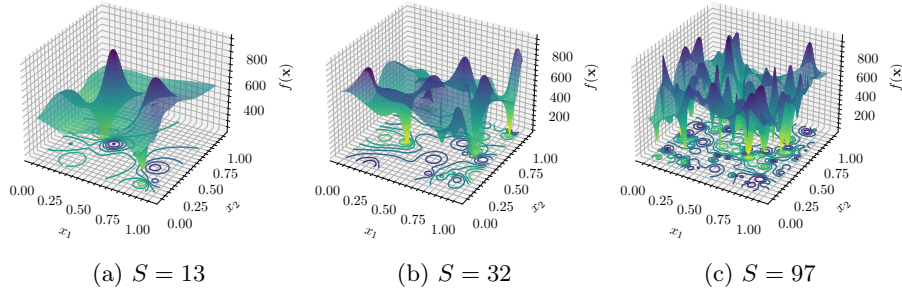


Fig. 4: Example of the first benchmark considered, S represents the number of stationary points.

2. Second Benchmark: it consists of objective functions generated using the methodology described in [41]. The original implementation was in C programming language, but we rewrote it in Python for our experiments. Similarly to the first benchmark, we considered 100 test functions for each dimension N ranging in

$\{2, 3, 4, 6, 8, 10\}$, resulting in a total of 600 different test functions. This benchmark involves several hyperparameters: the distance A from the global minimizer to the vertex of the paraboloid, the size of the basin of attraction B of the global minimizer, and the number of local minima C . To create a challenging benchmark, we randomly set A in the range $[0.8, 1)$, B in the range $[0.1, 0.2)$, and C from 3 to 10. These parameter settings ensure that the global minimizer is far from the vertex of the paraboloid and has a small basin of attraction.

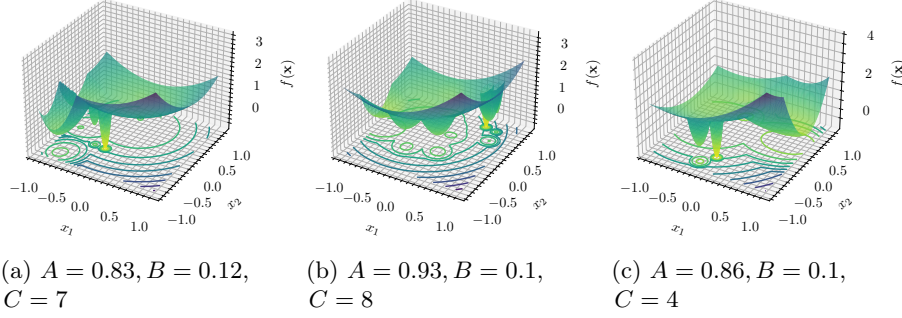


Fig. 5: Example of the second benchmark considered, A is the distance from the global minimizer to the vertex of the paraboloid, B the radius of the basin of attraction of the global minimizer and C the number of local minima.

3. Third Benchmark: it comprises popular test functions frequently used to evaluate the performance of both local and global optimization algorithms, such as the Rosenbrock, Beale, Michalewicz, and Hartmann functions, as defined in [46]. In total, we considered 191 different functions for this benchmark. When a test function is applicable to multiple dimensions N , we used the same function for different values of N ranging in $\{2, 3, 4, 6, 8, 10\}$. Therefore, the total number of experiments using this benchmark is 496. In cases where a function has its global minimum at the center of the domain, we randomly shifted the global minimizer within the domain.

5.1.3 Stopping Criteria

The termination criteria for our experiments are defined based on two conditions. Firstly, the relative error to the global optimal objective function value, denoted as f_{glob} , is used as a stopping criterion. The termination condition is satisfied when the following inequality holds

$$\frac{f - f_{\text{glob}}}{|f_{\text{glob}}|} \leq 10^{-4} \quad (34)$$

This condition ensures that the difference between the current objective function value (f) and the global optimal objective function value (f_{glob}) is within a small relative error tolerance of 10^{-4} .

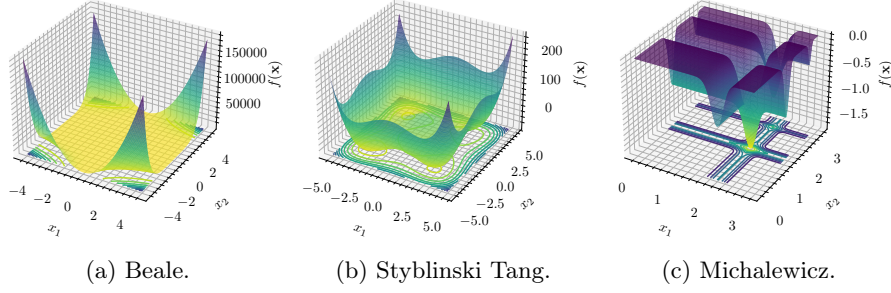


Fig. 6: Example of the third benchmark considered.

The second termination criterion is based on the maximum number of function evaluations. In our experiments, we fixed this limit to 10000, irrespective of the problem’s dimensionality. If an algorithm exceeds 10000 function evaluations without satisfying the criterion defined in Eq. 34, the run is considered to have failed.

These termination criteria provide a balance between achieving accurate solutions and limiting the computational effort. By combining the relative error criterion with a maximum number of function evaluations, we ensure that the algorithms converge within a reasonable computational budget.

5.2 Comparison Results and Discussion

In the following three subsections, we present and analyze the numerical results obtained by each algorithm for the benchmarks considered in this study.

Given the large number of objective functions in each benchmark, we will provide a summary of the results using operational characteristics [47], also known as performance profiles [48], along with tables. This approach allows us to effectively summarize and compare the performance of different algorithms across multiple test functions.

5.2.1 First Benchmark Results

Table 1 presents a summary of the numerical results obtained for the first benchmark. In terms of both the percentage of problems solved and the number of function evaluations, the best performing algorithm is HALO_{L-BFGS-B}, while the CMA-ES algorithm appears to be the least effective.

Notably, there is no significant difference in performance between the two versions of HALO equipped with different local optimizers. However, an interesting observation is the difference in performance between HALO_{SDBOX} and HLO. HALO_{SDBOX} solves 14.2% more problems than HLO and demonstrates a much faster convergence, as evident from the operational characteristic plot shown in Fig. 7a. Additionally, HLO performs worse than DIRECT. Upon analyzing this discrepancy, we found that HLO often selects only two hyperrectangles based on the estimate of the global Lipschitz constant. These hyperrectangles are the one with the minimum objective function value (selected apriori) and the hyperrectangle with the largest diagonal and lowest

objective function value. Consequently, if the global minimum is not within these two partitions, the overall convergence of the HLO algorithm is compromised.

In this benchmark, DIRMIN significantly accelerates the convergence of DIRECT. Particularly interesting is the performance of DIRMIN as the dimensionality of the problem varies, as shown in Fig. 8a. It can be observed that for $N \geq 6$, DIRMIN outperforms DIRECT, and for $N \geq 8$, it outperforms all the algorithms considered in this benchmark. This highlights that DIRMIN is less affected by the curse of dimensionality, possibly due to its effective utilization of the local optimization algorithm, which enables it to capture the local trends of the objective function.

Lastly, it is worth noting that CMA-ES often gets trapped in bad local minima for the majority of the objective functions, regardless of the problem’s dimensionality (see Fig. 8a). Table 1 reports the average percentage of solved problems for CMA-ES, along with the corresponding standard deviation in parentheses.

Table 1: Resume of the numerical results for the first benchmark.

Numerical results		
Algorithm	Percentage solved	Average functions evaluations
HALO _{L-BFGS-B}	74.1	1605.5
HALO _{SDBOX}	73.3	1655.3
HLO	59.1	1725.1
DIRMIN	69.5	1751.6
DIRECT	63.0	1762.8
CMA-ES	22.3 (1.3)	354.0

5.2.2 Second Benchmark Results

Table 2 presents a summary of the numerical results obtained in the second benchmark. In this case, the best performing algorithm is HALO_{SDBOX}, as it solves the highest percentage of problems. However, its performance is quite similar to HALO_{L-BFGS-B}, while the CMA-ES algorithm remains the least effective in this benchmark.

Our analysis indicates that this highly challenging benchmark evaluates the capability of a global optimization algorithm to efficiently explore the entire search space. An algorithm that overly emphasizes exploitation rather than exploration could struggle with many of the test functions in this benchmark. This is due to the small basin of attraction for the global minimum and the fixed relatively high distance from the vertex of the paraboloid (acting as a ‘trap’) to the global minimizer in all the test functions considered.

It is also interesting to analyze the difference between using the local Lipschitz constant, as in HALO_{SDBOX}, or the global Lipschitz constant, like in HLO. Additionally, this benchmark confirms that using an estimate of the local Lipschitz constant for each partition leads to better performance. HALO_{SDBOX} solves 3.2% more problems than HLO. When comparing the performance of DIRECT and its hybrid counterpart DIRMIN, it is evident that DIRMIN is significantly less effective than DIRECT. This

is primarily because too many local searches start and end up at the vertex of the paraboloid.

Finally, it appears that CMA-ES encounters significant difficulty in solving any of the objective functions. Our results indicate that almost 100% of the time, CMA-ES gets trapped at the vertex of the paraboloid.

Table 2: Resume of the numerical results for the second benchmark.

Numerical results		
Algorithm	Percentage solved	Average functions evaluations
HALO _{L-BFGS-B}	40.5	1877.5
HALO _{SDBOX}	40.8	1999.8
HLO	37.6	1946.8
DIRMIN	19.3	3392.5
DIRECT	31.6	1835.5
CMA-ES	10^{-3} (10^{-3})	10000

5.2.3 Third Benchmark Results

Table 3 provides a summary of the numerical results obtained in the third and final benchmarks. The HALO_{L-BFGS-B} algorithm emerges as the best performer, both in terms of the percentage of problems solved and the number of function evaluations. Conversely, the DIRECT algorithm appears to be relatively less effective.

There are noticeable performance differences between the two versions of HALO employing different local optimizers. The variant equipped with the gradient-based optimizer, HALO_{L-BFGS-B}, demonstrates greater efficiency, solving an average of 2% more problems with 100 fewer function evaluations compared to HALO_{SDBOX}. While HALO_{SDBOX} and HLO exhibit similar problem-solving capabilities, HALO_{SDBOX} achieves the solutions with an average of 200 fewer function evaluations than HLO. This confirms that in this benchmark, utilizing an estimate of the local Lipschitz constant accelerates the algorithm’s convergence towards the global minimizers more effectively than relying solely on the global Lipschitz constant. This observation is supported by the operational characteristics shown in Fig. 7c.

Although DIRMIN significantly accelerates the convergence of DIRECT, it does not outperform HALO and HLO. This is likely because DIRECT-type approaches, based on potentially optimal hyperrectangles, tend to sample a large number of them, leading to extensive exploration of sub-optimal regions in the domain \mathcal{D} . CMA-ES shows better performance compared to the DIRECT algorithm but remains less competitive compared to the other approaches considered.

Fig. 8c highlights the performance of all algorithms across varying dimensionalities N . It can be observed that HALO_{L-BFGS-B}, HALO_{SDBOX}, HLO, and DIRMIN exhibit similar performance across different dimensionalities. CMA-ES also shows similar performance, slightly underperforming for $N = 2$ but remaining competitive for

other values of N . On the other hand, DIRECT demonstrates a marked performance deterioration for $N \geq 6$ in this benchmark.

To further analyze the algorithm performances, we divided the functions in this benchmark into two groups. The first group consists of functions exhibiting a simple trend that attracts the algorithm towards a global minimizer, as shown in Fig. 9. The second group contains functions with more complex behavior, making it more challenging to locate the global minimizer, as shown in Fig. 10. The 'simple' group consists of 77 functions, while the 'hard' group consists of 116 functions.

Analyzing the operational characteristics in Fig. 11a and Fig. 11b, we can make several observations. Firstly, CMA-ES performs poorly on the hard functions but exhibits remarkable performance on the simple functions group. This suggests that CMA-ES focuses more on exploitation rather than exploration during the optimization process. Another interesting finding is the comparison between HLO and HALO_{SDBOX}. In the simple group, their performances are similar, but HALO_{SDBOX} outperforms HLO in the hard functions group. This indicates that when the objective function exhibits simple behavior, the information provided by the local Lipschitz constants used in HALO_{SDBOX} does not significantly improve performance compared to using only the global Lipschitz constant in HLO. However, when the objective function displays more chaotic behavior, the information from the local Lipschitz constant becomes highly valuable. Regarding the comparison between HALO_{L-BFGS-B} and HALO_{SDBOX}, as seen in Fig. 11a and Fig. 11b, the performance difference is minimal in the hard function group, while HALO_{L-BFGS-B} outperforms HALO_{SDBOX} in the simple function group. This suggests that the gradient-based local optimizer (L-BFGS-B) is more efficient than the derivative-free optimizer (SDBOX) when the objective function exhibits simple behavior. Finally, Fig. 12a and Fig. 12b illustrate that the DIRECT algorithm is more affected by the 'curse of dimensionality' phenomenon compared to the other approaches.

Table 3: Resume of the numerical results for the third benchmark.

Algorithm	Numerical results	
	Percentage solved	Average functions evaluations
HALO _{L-BFGS-B}	72.9	776.8
HALO _{SDBOX}	70.1	842.2
HLO	69.1	1015.6
DIRMIN	67.1	965.7
DIRECT	61.2	1315.9
CMA-ES	65.2 (1.0)	898.9

5.2.4 Parameter Sensitivity Analysis

In this section, we will analyze the impact of different choices for the parameter β on the performance of HALO. The parameter β is used in Eq. 19 to determine whether a partition \mathcal{D}_{i_k} is small enough to consider its centroid as a starting point for the local

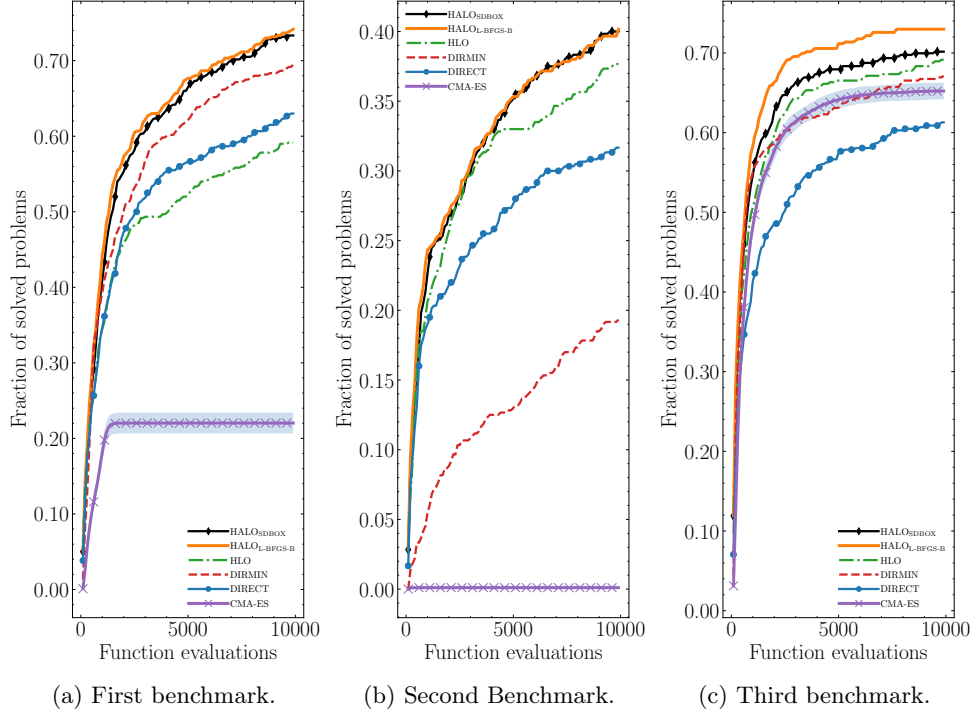


Fig. 7: Operational characteristics for the three benchmarks.

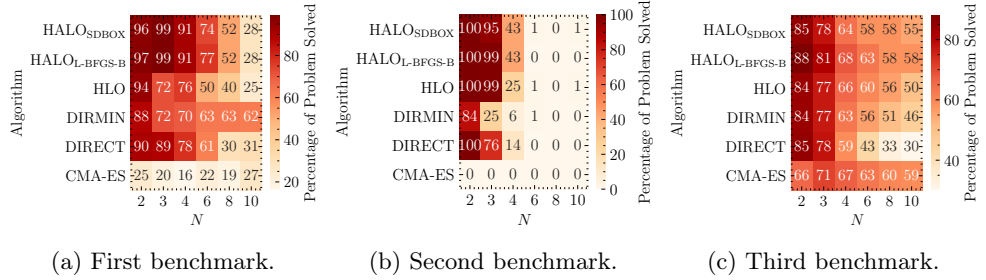


Fig. 8: Percentage of the problem solved varying the dimensionality N .

optimizer. A small value of β will result in HALO using the local optimizer infrequently, while a higher value will make HALO rely more heavily on the local optimizer. However, it is important to be cautious when selecting a high value for β because once the local search starts from the centroid of a partition, that partition will never be further partitioned in the future as described in Section 4.3. We conducted experiments using

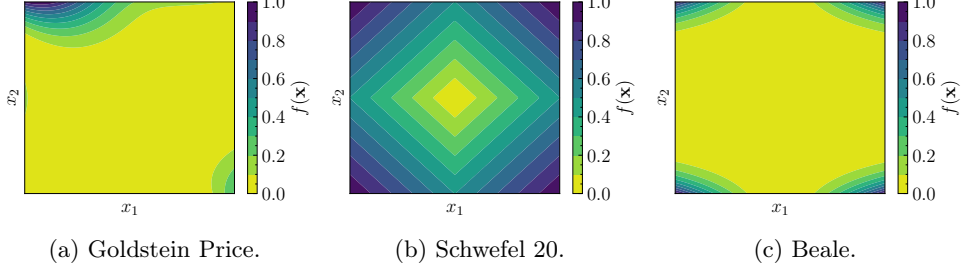


Fig. 9: Simple functions belonging in the third benchmark. Function values are normalized.

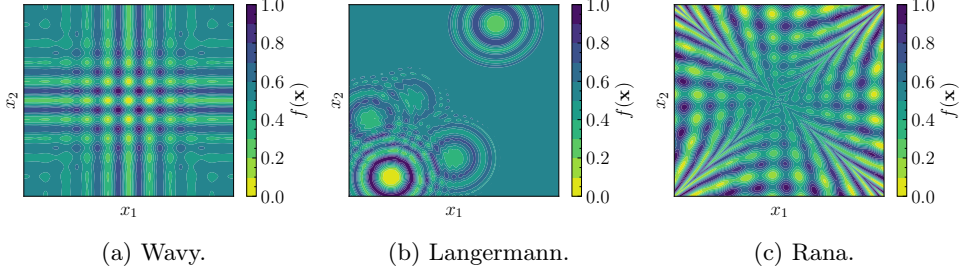


Fig. 10: Hard functions belonging is the third benchmark. Function values are normalized.

HALO_{L-BFGS-B} and HALO_{SDBOX} with various values of β in the range

$$\beta \in \{10^{-1}, 10^{-2}, 10^{-3}, 10^{-4}, 10^{-5}, 10^{-6}\} \quad (35)$$

for all the functions in the three different benchmarks. The results are summarized in Table 4.

In general, the performance of HALO appears to be quite robust with respect to the choice of the parameter β , particularly for β values between 10^{-2} and 10^{-6} . This observation is supported by the operational characteristics shown in Fig. 13a and Fig. 13b for HALO_{L-BFGS-B} and HALO_{SDBOX}, respectively. Moreover, within the range of β values from 10^{-2} to 10^{-6} , the choice of the local optimizer (L-BFGS-B or SDBOX) does not significantly affect the performance of HALO. Although HALO_{L-BFGS-B} demonstrates the best performance in terms of average function evaluations and percentage of problems solved, the difference in performance between HALO_{SDBOX} and HALO_{L-BFGS-B} is not substantial.

Table 4 also presents the average number of local optimization routines initiated varying β . On average, one or two local optimization routines start when $\beta \in [10^{-3}, 10^{-6}]$ or when $\beta = 10^{-2}$, respectively, for both HALO_{SDBOX} and HALO_{L-BFGS-B}. However, the

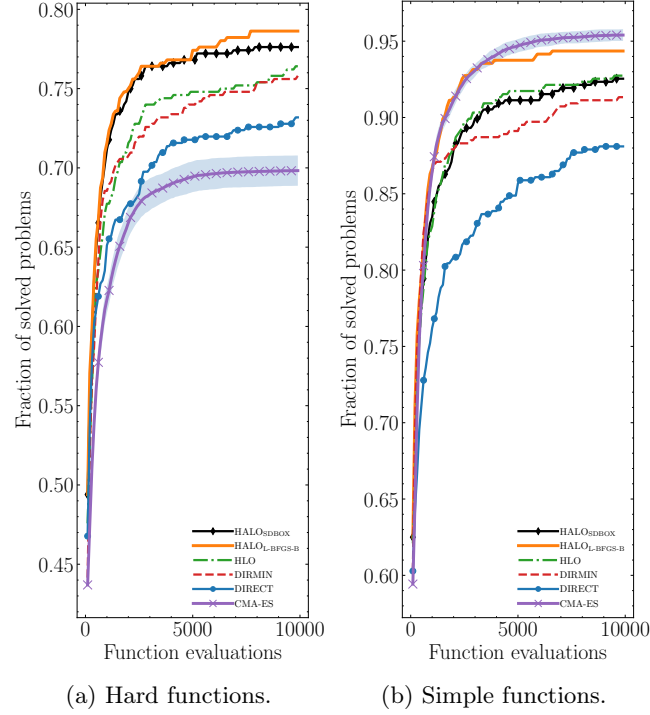


Fig. 11: Operational characteristics for the two groups (hard and simple) of functions belonging to the third benchmark.

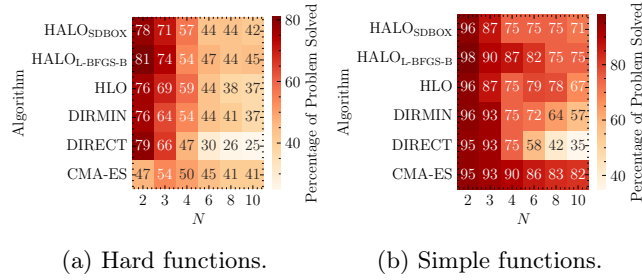


Fig. 12: Percentage of problems solved varying the dimensionality N for the two groups (hard and simple) of functions belonging to the third benchmark.

situation changes when $\beta = 10^{-1}$, as both HALO_{SDBOX} and HALO_{L-BFGS-B} experience a performance decline, especially for $N = 3$ dimensions (see Fig. 14).

Based on the results, we recommend the following regarding the choice of β :

- Avoid selecting a value of β less than 10^{-4} to prevent HALO from consuming excessive function evaluations on very small hyperrectangles and to avoid potential numerical instabilities.
- If the objective function is expected to contain noise, we recommend using the derivative-free version of HALO, namely HALO_{SDBOX}, with β values between 10^{-2} and 10^{-4} . Otherwise, HALO_{L-BFGS-B} should be the default choice, again with β values between 10^{-2} and 10^{-4} .

Table 4: Resume of the numerical results for the sensitivity analysis with respect to the parameter β .

Numerical results						
β	Percentage solved		Average functions evaluations		Average n° local searches	
	HALO _{L-BFGS-B}	HALO _{SDBOX}	HALO _{L-BFGS-B}	HALO _{SDBOX}	HALO _{L-BFGS-B}	HALO _{SDBOX}
10^{-1}	60.0	60.0	1303.2 (2038.6)	1600.3 (2249.4)	3.6 (6.3)	3.4 (6.1)
10^{-2}	61.3	60.6	1310.8 (1939.5)	1493.7 (2042.4)	1.9 (2.4)	1.8 (2.4)
10^{-3}	61.4	60.2	1332.3 (1957.9)	1469.2 (2053.0)	1.3 (0.9)	1.3 (0.9)
10^{-4}	61.7	60.7	1394.3 (2034.7)	1442.5 (2005.6)	1.0 (0.8)	1.0 (0.8)
10^{-5}	61.3	60.7	1411.0 (2025.5)	1484.3 (2061.5)	1.0 (0.8)	0.9 (0.8)
10^{-6}	61.3	60.7	1414.5 (1995.7)	1524.4 (2102.5)	0.9 (0.8)	0.9 (0.8)

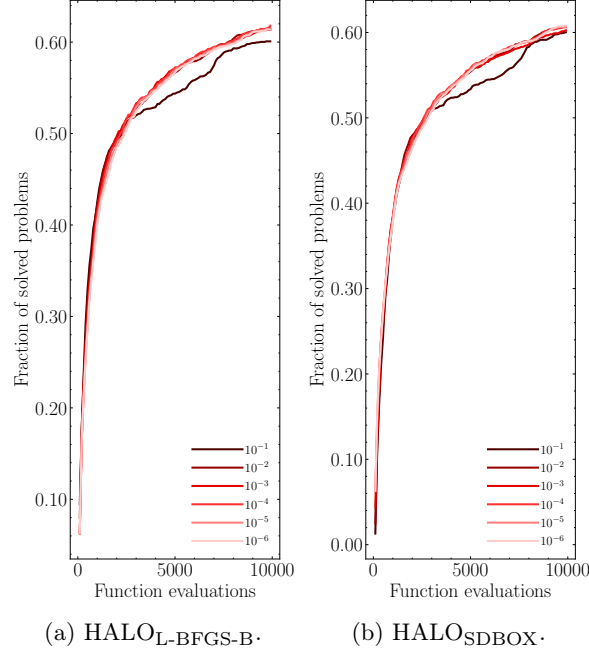
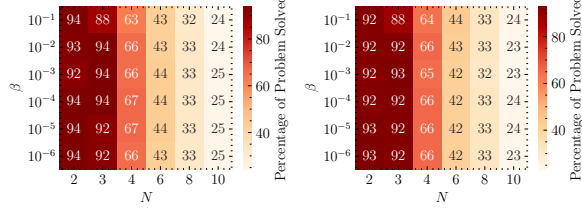
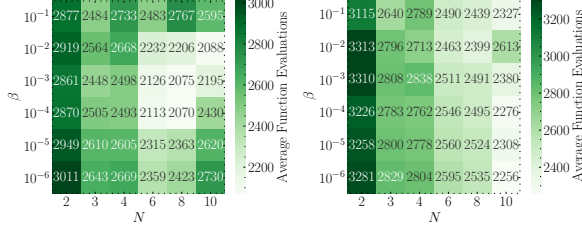


Fig. 13: Operational characteristics for the two versions of HALO.



(a) HALO_L-BFGS-B. (b) HALO_{SDBOX}.

Fig. 14: Percentage of problems solved varying the dimensionality N .



(a) HALO_L-BFGS-B. (b) HALO_{SDBOX}.

Fig. 15: Average number of functions evaluations varying the dimensionality N .

5.2.5 Highlighting the Variable Importance and Problem Interpretability

In addition to its optimization capabilities, HALO offers the potential for extracting valuable insights from the black-box objective function under consideration. In many practical applications, it is not only important to identify the global minimum but also to gain a deeper understanding of the variables that significantly impact the reduction of the objective function. Traditionally, such insights are obtained through sensitivity analysis, which involves computing gradients of the objective function. However, this process can be time-consuming, especially when dealing with computationally expensive simulations.

With HALO, we have an alternative approach to extracting similar information without the need for explicit and additional gradient computations. Once the optimization routine is completed, we can analyze the matrix \mathbf{G} (introduced in Section 4.5), which collects the vectors $\tilde{\nabla}f(\mathbf{x}_{i_k})$ around each centroid \mathbf{x}_{i_k} . By examining this matrix, we can gain insights into the directions in which the objective function exhibits greater sensitivity during the iterations of HALO. We can simply determine the variable importance by averaging the rows $\tilde{\nabla}f(\mathbf{x}_{i_k})$ of the matrix \mathbf{G} . This can be expressed as

$$\text{Variable Importance} = \frac{1}{|\mathcal{I}_k|} \sum_i^{|\mathcal{I}_k|} \tilde{\nabla}f(\mathbf{x}_{i_k}) \quad (36)$$

we also apply a final normalization step so that the variable importance vector sums to one.

In Fig. 16, we provide an illustrative example of the variable importance for three different objective functions: Eggholder, Dixon Price, and Adjiman respectively in Fig. 16a, 16b, and 16c. By examining the variable importance defined in Eq. 36, we can observe that it accurately identifies the directions in which the objective function exhibits the most significant variation.

This information can be valuable in understanding the underlying dynamics of the objective function and identifying the variables that have the most significant influence on its behavior. This knowledge not only enhances our understanding of the problem but can also guide further investigations, inform decision-making processes, and potentially lead to improvements in the optimization problem formulation or solution strategies.

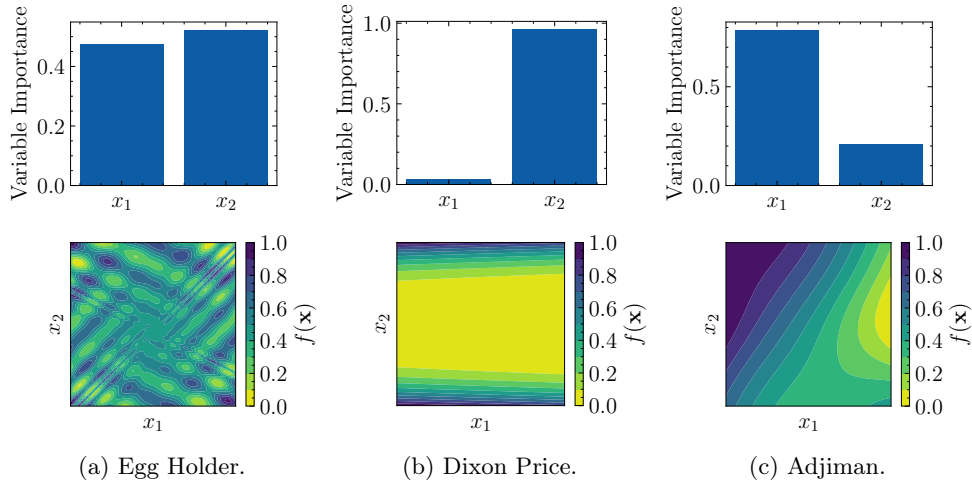


Fig. 16: Summary of the variable importance computed for various objective functions, extracted from HALO at the end of its iterations. The first row of figures shows the variable importance while in the second row the related objective function.

Compared to traditional sensitivity analysis techniques, leveraging the information available in \mathbf{G} from HALO offers several advantages. First, it eliminates the need for additional gradient computations, saving computational time and resources, particularly when dealing with computationally expensive simulations. Second, it provides insights specific to the optimization process, capturing the dynamics and patterns observed during the search for the global minimum.

6 Conclusions

In this study, we introduced HALO (Hybrid Adaptive Lipschitzian Optimization), a deterministic partition-based Global Optimization algorithm. HALO incorporates an

adaptive procedure to estimate the local Lipschitz constant for each partition or sub-region \mathcal{D}_i within the box domain \mathcal{D} . The estimation is performed automatically based on the size of the partition, eliminating the need for the user to define crucial hyperparameters in advance. The adaptive procedure strikes a balance between the current estimate of the global Lipschitz constant and the norm of the gradient approximation associated with the centroids of each partition.

We proposed a simple coupling strategy with local optimization algorithms to expedite the convergence towards a stationary point. By leveraging local optimization techniques, HALO achieves faster convergence speeds, enhancing its effectiveness in solving optimization problems.

To evaluate the performance of HALO, we conducted a comprehensive comparison with popular GO algorithms using three diverse benchmarks comprising numerous test functions. The results demonstrated that HALO exhibited robust performance across different problem domains. Additionally, we conducted a sensitivity analysis on a hyperparameter controlling the local search, and the findings indicated that HALO’s performance remains consistent within a certain range of hyperparameter values.

HALO not only enables efficient global optimization but also facilitates the extraction of valuable insights from the objective function. By analyzing the matrix that collects the approximation of the gradients around each partition’s centroid, we can identify the influential directions in the search space and gain a deeper understanding of the factors driving the reduction of the objective function. This feature makes HALO a powerful tool not only for optimization but also for exploratory analysis and problem understanding in a wide range of applications.

Based on these results, HALO emerges as highly competitive and can extend our tools of methodologies for tackling complex real-world GO problems. Its deterministic nature, lack of crucial hyperparameters to set, and integration with local optimization methods position HALO as a valuable addition to the toolbox of optimization practitioners.

References

- [1] Price, W.L.: A controlled random search procedure for global optimisation. *The Computer Journal* **20**(4), 367–370 (1977)
- [2] Davis, L.: *Handbook of Genetic Algorithms*. Chapman & Hall, London, UK (1991)
- [3] Johnson, D.S., Aragon, C.R., McGeoch, L.A., Schevon, C.: Optimization by simulated annealing: An experimental evaluation; part i, graph partitioning. *Operations research* **37**(6), 865–892 (1989)
- [4] Kennedy, J., Eberhart, R.: Particle swarm optimization. In: *Proceedings of ICNN’95-International Conference on Neural Networks*, vol. 4, pp. 1942–1948 (1995). IEEE
- [5] Hansen, N., Ostermeier, A.: Completely derandomized self-adaptation in evolution strategies. *Evolutionary computation* **9**(2), 159–195 (2001)

- [6] Jones, D.R., Schonlau, M., Welch, W.J.: Efficient global optimization of expensive black-box functions. *Journal of Global optimization* **13**(4), 455–492 (1998)
- [7] Mockus, J., Tiesis, V., Zilinskas, A.: The application of bayesian methods for seeking the extremum. *Towards global optimization* **2**(117-129), 2 (1978)
- [8] Gutmann, H.-M.: A radial basis function method for global optimization. *Journal of global optimization* **19**(3), 201–227 (2001)
- [9] Regis, R.G., Shoemaker, C.A.: A stochastic radial basis function method for the global optimization of expensive functions. *INFORMS Journal on Computing* **19**(4), 497–509 (2007)
- [10] Horst, R., Tuy, H.: *Global Optimization: Deterministic Approaches*. Springer, Berlin, Heidelberg (2013)
- [11] Horst, R., Pardalos, P.M.: *Handbook of Global Optimization vol. 2*. Springer, Berlin, Heidelberg (2013)
- [12] Sergeyev, Y.D., Kvasov, D.E.: Global search based on efficient diagonal partitions and a set of lipschitz constants. *SIAM Journal on Optimization* **16**(3), 910–937 (2006)
- [13] Törn, A., Žilinskas, A.: *Global Optimization*. Springer, Berlin, Heidelberg (1989)
- [14] Pintér, J.D.: *Global Optimization in Action: Continuous and Lipschitz Optimization: Algorithms, Implementations and Applications vol. 6*. Springer, Berlin, Heidelberg (1995)
- [15] Paulavičius, R., Žilinskas, J.: Analysis of different norms and corresponding lipschitz constants for global optimization in multidimensional case. *Information Technology and Control* **36**(4) (2007)
- [16] Shubert, B.O.: A sequential method seeking the global maximum of a function. *SIAM Journal on Numerical Analysis* **9**(3), 379–388 (1972)
- [17] Mladineo, R.H.: An algorithm for finding the global maximum of a multimodal, multivariate function. *Mathematical Programming* **34**(2), 188–200 (1986)
- [18] Jones, D.R., Perttunen, C.D., Stuckman, B.E.: Lipschitzian optimization without the Lipschitz constant. *Journal of Optimization Theory and Applications* **79**(1), 157–181 (1993)
- [19] Gablonsky, J.M., Kelley, C.T.: A locally-biased form of the direct algorithm. *J. of Global Optimization* **21**(1), 27–37 (2001) <https://doi.org/10.1023/A:1017930332101>
- [20] Mockus, J.: On the pareto optimality in the context of lipschitzian optimization.

- [21] Paulavičius, R., Sergeyev, Y.D., Kvasov, D.E., Žilinskas, J.: Globally-biased direct algorithm with local accelerators for expensive global optimization. *Expert Systems with Applications* **144**, 113052 (2020)
- [22] Mockus, J., Paulavičius, R., Rusakevičius, D., Šešok, D., Žilinskas, J.: Application of reduced-set pareto-lipschitzian optimization to truss optimization. *Journal of Global Optimization* **67**(1-2), 425–450 (2017)
- [23] Liu, Q., Zeng, J., Yang, G.: Mrdirect: a multilevel robust direct algorithm for global optimization problems. *Journal of Global Optimization* **62**(2), 205–227 (2015)
- [24] Liu, Q., Yang, G., Zhang, Z., Zeng, J.: Improving the convergence rate of the direct global optimization algorithm. *Journal of Global Optimization* **67**(4), 851–872 (2017)
- [25] Lera, D., Sergeyev, Y.D.: Deterministic global optimization using space-filling curves and multiple estimates of lipschitz and hölder constants. *Communications in Nonlinear Science and Numerical Simulation* **23**(1-3), 328–342 (2015)
- [26] Paulavičius, R., Žilinskas, J.: Simplicial lipschitz optimization without lipschitz constant. In: *Simplicial Global Optimization*, pp. 61–86. Springer, Berlin, Heidelberg (2014)
- [27] Sergeyev, Y.D.: An information global optimization algorithm with local tuning. *SIAM Journal on Optimization* **5**(4), 858–870 (1995)
- [28] Strongin, R.G.: Algorithms for multi-extremal mathematical programming problems employing the set of joint space-filling curves. *Journal of Global Optimization* **2**(4), 357–378 (1992)
- [29] Sergeyev, Y.D., Strongin, R.G., Lera, D.: *Introduction to Global Optimization Exploiting Space-filling Curves*. Springer, Berlin, Heidelberg (2013)
- [30] Kvasov, D.E., Pizzuti, C., Sergeyev, Y.D.: Local tuning and partition strategies for diagonal go methods. *Numerische Mathematik* **94**(1), 93–106 (2003)
- [31] Gergel, V., Grishagin, V., Israfilov, R.: Local tuning in nested scheme of global optimization. *Procedia Computer Science* **51**, 865–874 (2015)
- [32] Gergel, V., Grishagin, V., Gergel, A.: Adaptive nested optimization scheme for multidimensional global search. *Journal of Global Optimization* **66**(1), 35–51 (2016)
- [33] Gergel, V.P.: A global optimization algorithm for multivariate functions with lipschitzian first derivatives. *Journal of Global Optimization* **10**(3), 257–281 (1997)

- [34] Jones, D.R., Martins, J.R.: The direct algorithm: 25 years later. *Journal of Global Optimization*, 1–46 (2020)
- [35] Liuzzi, G., Lucidi, S., Piccialli, V.: A direct-based approach exploiting local minimizations for the solution of large-scale global optimization problems. *Computational Optimization and Applications* **45**(2), 353–375 (2010)
- [36] Liuzzi, G., Lucidi, S., Piccialli, V.: Exploiting derivative-free local searches in direct-type algorithms for global optimization. *Computational Optimization and Applications* **65**(2), 449–475 (2016)
- [37] Byrd, R.H., Lu, P., Nocedal, J., Zhu, C.: A limited memory algorithm for bound constrained optimization. *SIAM Journal on scientific computing* **16**(5), 1190–1208 (1995)
- [38] Lucidi, S., Sciandrone, M.: A derivative-free algorithm for bound constrained optimization. *Computational Optimization and Applications* **21**(2), 119–142 (2002)
- [39] Jamil, M., Yang, X.S.: A literature survey of benchmark functions for global optimisation problems. *International Journal of Mathematical Modelling and Numerical Optimisation* **4**(2), 150 (2013) <https://doi.org/10.1504/ijmmno.2013.055204>
- [40] Schoen, F.: A wide class of test functions for global optimization. *Journal of Global Optimization* **3**(2), 133–137 (1993)
- [41] Gaviano, M., Kvasov, D.E., Lera, D., Sergeyev, Y.D.: Software for Generation of Classes of Test Functions with Known Local and Global Minima for Global Optimization (2011)
- [42] Di Pillo, G., Liuzzi, G., Lucidi, S., Piccialli, V., Rinaldi, F.: A direct-type approach for derivative-free constrained global optimization. *Computational Optimization and Applications* **65**(2), 361–397 (2016)
- [43] D’Agostino, D., Serani, A., Diez, M.: On the combined effect of design-space dimensionality reduction and optimization methods on shape optimization efficiency. In: 19th AIAA/ISSMO Multidisciplinary Analysis and Optimization Conference (MA&O), AVIATION 2018, Atlanta, GA, USA, June 25-29 (2018)
- [44] Hansen, N., Auger, A., Ros, R., Finck, S., Pošík, P.: Comparing results of 31 algorithms from the black-box optimization benchmarking bbob-2009. In: Proceedings of the 12th Annual Conference Companion on Genetic and Evolutionary Computation, pp. 1689–1696 (2010)
- [45] Cassioli, A., Schoen, F.: Global optimization of expensive black box problems with a known lower bound. *Journal of Global Optimization* **57**(1), 177–190 (2013)

- [46] Jamil, M., Yang, X.S.: A literature survey of benchmark functions for global optimisation problems. *International Journal of Mathematical Modelling and Numerical Optimisation* **4**(2), 150 (2013) <https://doi.org/10.1504/ijmmno.2013.055204>
- [47] Strongin, R.G., Sergeyev, Y.D.: *Global Optimization with Non-convex Constraints: Sequential and Parallel Algorithms* vol. 45. Springer, Berlin, Heidelberg (2013)
- [48] Dolan, E.D., Moré, J.J.: Benchmarking optimization software with performance profiles. *Mathematical programming* **91**(2), 201–213 (2002)